JOURNAL OF PHYSICAL ORGANIC CHEMISTRY
J. Phys. Org. Chem. 2005; **18:** 240–249
Published online 21 July 2004 in Wiley InterScience (www.interscience.wiley.com). DOI: 10.1002/poc.840

Restricted rotation/tautomeric equilibrium and determination of the site and extent of protonation in bi-imidazole nucleosides by multinuclear NMR and GIAO-DFT calculations

Jukka Mäki,[1] Petri Tähtinen,[2] Leif Kronberg[1] and Karel D. Klika[2]*

[1]Department of Organic Chemistry, Åbo Akademi University, Biskopsgatan 8, FIN-20500 Åbo, Finland
[2]Structural Chemistry Group, Department of Chemistry, University of Turku, Vatselankatu 2, FIN-20014 Turku, Finland

Received 16 March 2004; revised 6 May 2004; accepted 11 May 2004

ABSTRACT: The restricted rotation about the conjoining bond in a series of 4″-substituted bi-imidazole nucleosides {5-amino-4-[4″-R-imidazol-2″-yl]-1-(β-D-ribofuranosyl)-1*H*-imidazole; where R = H, methyl, hydroxymethyl, oxalo, formyl} due to intramolecular hydrogen bonding between N-3″ and the N-6 protons concomitant with prototropic tautomerism has been examined using multinuclear (^{1}H, ^{13}C and ^{15}N) experimental NMR. Substitution at the 4″ position causes the interconversion, whilst still an intramolecular process, to yield complex spectra as the dynamic process consists of a two-site exchange between non-degenerate tautomeric forms (asymmetric sites). The preferred tautomers were identified experimentally in each case and compared with theoretically determined structures geometry optimized using density functional theory (DFT) at the B3LYP/6–31G(d,p) level of theory on which gauge-independent atomic orbital-DFT (GIAO-DFT) computations at the B3LYP/cc-pVTZ level of theory were applied to calculate the chemical shifts of the ^{1}H, ^{13}C and ^{15}N nuclei. Both the site and the extent of protonation of the bi-imidazole nucleosides were also similarly ascertained using the same methodology. Protonation at the pyridine-type nitrogen (N-3″) of the outer imidazole ring, the principle site of protonation, effectively eliminated the barrier to rotation about the conjoining bond yielding time-averaged spectra experimentally. Copyright © 2004 John Wiley & Sons, Ltd.
Supplementary electronic material for this paper is available in Wiley Interscience at http://www.interscience.wiley.com/jpages/0894-3230/suppmat/

KEYWORDS: NMR spectroscopy; molecular modeling; DFT calculations; etheno adducts; tautomeric equilibrium; hindered rotation

INTRODUCTION

The study of DNA structural modifications (lesions) and their repair mechanisms continues to receive considerable attention[1] due to their prominent role in mutations, aging and in degenerative diseases associated with aging, e.g. cancer.[2] Some of the most commonly encountered DNA lesions are the exocyclic DNA adducts and, in particular, etheno adducts with an additional five-membered ring fused to the base moiety are of considerable interest[3] since they can result from reaction with a variety of chemicals,[4] can exhibit miscoding properties[5] and can persist in some tissues.[6] For example, the 1,N^6-ethenoadenosine adducts depicted in Scheme 1 have been reported[4,7] as a result of the reaction of genotoxic agents with adenosine. The etheno adducts are not necessarily stable and can react further; for example, in basic aqueous solution 1,N^6-ethenoadenosine and its substituted derivatives form the bi-imidazole nucleosides **1** and **3–5** by ring-opening and subsequent deformylation.[8,9]

Despite the present level of spectroscopic analysis, confusion can still exist for structural motifs of fairly basic simplicity, such as represented by these imidazole moieties, and even recently workers have highlighted a number of inconsistencies in the NMR signal assignments of imidazoles.[9,10] However, there are several factors that can account for these anomalies, *viz*. the state of protonation, the existence of tautomeric equilibrium, and the peculiarities of the scalar coupling constants that can occur either wholly within or incorporating a five-membered ring (e.g. $^{3,4}J_{H,H}$, $^{2,3}J_{H,C}$, $^{11\ 2-4}J_{H,N}$,[12]). Of the many methods available for determining the state of protonation, only a few can definitively indicate the actual site of protonation within the molecule. Despite its limited sensitivity, ^{15}N NMR is one of the preferred methods[13,14] for such studies and therefore also for the study of valence and prototropic tautomerism.[14,15] The concept of protonation site and the determination of it by NMR has been well reviewed.[16]

**Correspodnence to:* Dr. K. D. Klika, Department of Chemistry, University of Turku, Vatselankatu 2, FIN-20014 Turku, Finland.
E-mail: karel.klika@utu.fi

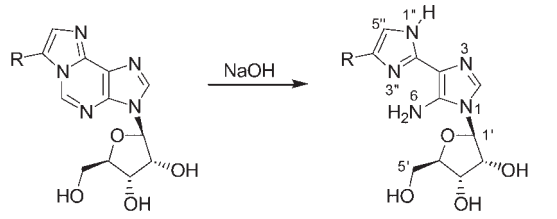

Scheme 1. The ring opening of the 1,N^6-ethenoadenosine adducts to yield the bi-imidazole nucleosides **1**–**5**. The atom labelling in use for compounds **1**–**5** is indicated

In a previous study in which the restricted rotation and concomitant prototropic tautomerism of **1** were reported,[14] the basis for the restricted rotation about the C_4—$C_{2''}$ bond adjoining the two imidazole rings was the intramolecular hydrogen bonding that was in effect between the N-6 protons and N-3″ resulting in two degenerate forms, **1a** and **1d** (see Scheme 2). Protonation of **1** at N-3″ (**1H**), as indicated by the large chemical shift change of N-3″, resulted in the reduction of the intramolecular hydrogen bonding and essentially free rotation about the C_4—$C_{2''}$ bond. Upon substitution, the situation is rendered more complex and the study is now extended to encompass the results of such substitution and include

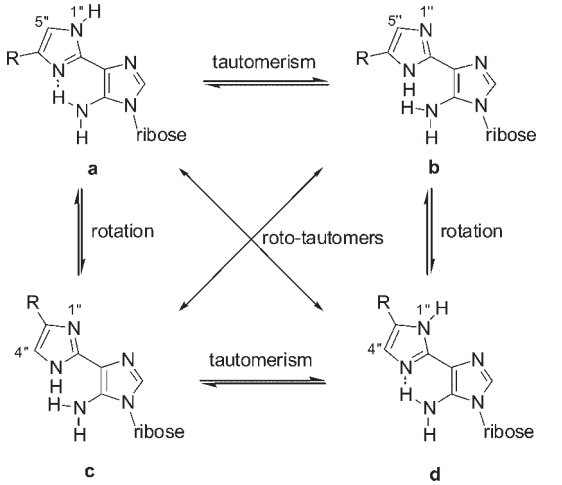

Scheme 2. The interconversion by prototropic tautomerism and/or rotation between various structures for the non-protonated species **1**–**5** showing, where applicable, the hydrogen bonding that is in effect and responsible for the restricted rotation about the C_4——$C_{2''}$ bond. The numbering of the nitrogens defined in the outer bi-imidazole moiety, for the sake of clarity, remains invariant in ensuing tautomeric conversions, i.e. the number of the nitrogens are spatially fixed and the nitrogen farthest from N-6 is always labelled N-1″ even though this results in an unconventional numbering for structures **b** and **c**

the newly synthesized, methyl-substituted **2** as well as the previously reported[9] compounds **3**–**5** together with their protonated forms **1H**–**5H**. As before,[14] the results of this study rely principally on ^{15}N NMR but the experimental results are now supported by theoretical calculations of the chemical shifts of the ^{1}H, ^{13}C and ^{15}N nuclei using gauge-independent atomic orbital[17]-density functional theory[18] (GIAO-DFT) methods on theoretically determined structures geometry optimized using DFT at the B3LYP/6–31G(d,p) level of theory.

RESULTS AND DISCUSSION

The assignment of the resonances and the structures themselves of compounds **1**–**5** were based mostly on the standard application of COSY and HMQC together with a heavy reliance on ^{1}H{^{13}C} and ^{1}H{^{15}N} HMBC experiments, but in some instances on comparison with previous assignments, chemical shifts, or ultimately, by default. For both ^{13}C and ^{15}N NMR, despite ample quantities of sample, detection difficulties were occasionally encountered in the cases of extreme exchange broadening and as a consequence, spectra were also acquired at higher temperatures. For ^{1}H{^{15}N} HMBC correlations, the $^2J_{H,N}$ couplings were assumed to be larger, and therefore the correlations expected to be more pronounced, in comparison to the $^3J_{H,N}$ couplings within the imidazole rings.[12] Although both ^{13}C and ^{1}H are also potential indicators of the site of protonation, both nuclei are sensitive to structural changes and, additionally for ^{1}H, also subject to general environment changes. In this work, the chemical shifts of the ^{1}H nuclei were, on occasion, concentration dependent but, surprisingly, not that temperature dependent. ^{13}C and ^{15}N spectra (both only measured for concentrated samples) were also found to be fairly insensitive to temperature. Overall, the ^{1}H chemical shifts were not particularly indicative, despite the fact that the chemical shifts of the protons neighbouring the protonation site (i.e. H-2, H-5′) can move to lower field by as much as 1 ppm.[19] Of the carbons, the most indicative was C-4 which moves noticeably upfield upon protonation of N-3′, N-3, or both.

For calculation of the chemical shifts, refinement of the geometries was first performed by a hybrid DFT[18] method at the B3LYP/6–31G(d,p) level of theory in order to define the structures at a sufficiently high level of theory appropriate[20] for the calculation of reliable NMR shielding constants. For the various calculated conformations, the input geometries predetermined the structures with respect to rotation about the C_4—$C_{2''}$ bond. Systematic conformational searching of the ribose unit was not performed as the chemical shifts of the bi-imidazole moiety are not substantially affected by changes in the sugar ring and the same ribose conformation was thus maintained throughout. The energy of each geometry-optimized structure was also calculated at the

same level of theory. The nuclear shieldings were calculated using the GIAO method[17] at the B3LYP/cc-pVTZ level of theory. For scaling of the calculated chemical shifts (^{15}N, ^{13}C and ^{1}H), a broad range of different compounds were used for calibration (ca 25 in total, see Experimental). Although the calibration for each of the three nuclei (see Figs 1–3 for ^{15}N, ^{13}C and ^{1}H nuclei, respectively) using these compounds all resulted in very good correlations ($R^2 = 0.992$, 0.999 and 0.997 for ^{15}N, ^{13}C and ^{1}H nuclei, respectively), significant deviations for the chemical shifts in terms of chemical interpretation were often encountered, but nevertheless trends were still in evidence and are discussed on a case-by-case basis.

5-Amino-4-imidazol-2″-yl-1-(β-D-ribofuranosyl)-1*H*-imidazole (1)

As reported previously[14] for the unsubstituted compound **1** (see Table S1 for the ^{15}N and ^{13}C chemical shifts and Table S2 for the ^{1}H chemical shifts of the imidazole rings and attendant R substituent in EPOC), of the four possible identifiable species related by either prototropic shifts or rotation about the C_4—$C_{2''}$ bond, restricted rotation about the C_4—$C_{2''}$ bond was observed but concomitant with rotation was prototropic tautomerism. Thus, species **1b** and **1c** resulting only from rotation or tautomerism were not detected as discrete entities and only the two, spin-indistinguishable species **1a** and **1d** were in evidence by NMR, i.e. the interconversion amounts to an intramolecular dynamic process consisting of symmetrical two-site exchange. Given the dual nature of the interconversion between **1a** and **1d**, the term 'roto-tautomers' is applied to the two species **1a** and **1d** (and similarly, **1b** and **1c**). The basis for the restricted rotation, and the reason why structure **1a** (**1d**) is preferred over **1b** (**1c**), is the favourable intramolecular hydrogen bonding that occurs between the N-6 protons and N-3″ in **1a**. Consistent with this, the two planes of the imidazole rings were calculated to be effectively coplanar in **1a** (see Table S2), i.e. facile delocalization of the π electrons between the two rings can be assumed to be in effect. For **1b**, two energy minimum structures were located, **1b′** and **1b″**. In the former case, the N-6 protons are orientated towards H-3″ and the steric hindrance that results is only alleviated by the twisting of the imidazole rings, i.e. rotation about the C_4—$C_{2''}$ bond (a torsion angle of 34.25° was calculated), with the consequent loss of the facile delocalization. The cost is effectively seen in the raised energy of the system, 58 kJ mol^{-1} higher relative to **1a** (Table S2). The other structure, **1b″**, has the N-6 protons orientated away from H-3″ and this not only eliminates the steric repulsion, but permits hydrogen bonding to be in effect between H-3″ and N-6, i.e. in the reverse order to that in operation in **1a**. But the removal of an unfavourable interaction and the introduction of a favourable interaction does not translate into an energetically preferred species as these benefits appear to be offset by a detrimental change in the electron distribution of the imidazole rings (as indicated by the chemical shifts of N-1, N-3 and C-4) brought about by the reverse order of the hydrogen bonding. Thus a high energy species results as well, coincidentally also 58 kJ mol^{-1} higher relative to **1a**. These changes do, nonetheless, permit the return of near co-planarity of the two imidazole rings in **1b″** (calculated torsion angle of 5.69°). The differences in the calculated chemical shifts (also included in Tables S1 and S2) between **1b′** and **1b″** bear out these structural changes, e.g. the chemical shift of the H-6s were calculated to be 1.8 ppm more downfield in **1b′**, which can be ascribed to both steric compression and hydrogen bonding effects, similarly the calculated downfield shift of H-3″ in **1b″** (+2.6 ppm) can be attributed solely to the hydrogen bonding that this proton is engaged in. On the ^{13}C and ^{15}N side, there are many changes due to electronic redistribution with the most significant noted above, but in addition the relative upfield position of N-3″ in **1b′** (−3.5 ppm) can be ascribed to steric compression effects and the downfield position of N-6 in **1b′** (+12.4 ppm) due to loss of hydrogen bonding in this structure. With an energy difference of 58 kJ mol^{-1}, the concentration of species **1b** is thus inferred to be negligible under the experimental conditions.

The calculated ^{1}H chemical shifts for structures **1a** and **1b** provided little assistance in assessing the preferred roto-tautomer, but the ^{13}C and ^{15}N chemical shifts on the whole saw fair agreement between the experimental values and those calculated for structure **1a** in comparison with those of structure **1b**. The most dramatic example was N-3 where the calculated values differed by almost 20 ppm and the experimental value was within 2.66 ppm of the value calculated for structure **1a**. In some cases even structure **1b** was favourably implicated by the chemical shifts, notably by the chemical shift of N-6, but on the whole, confidence in the agreement between the calculated values for the known structure **1a** and the experimental values was high and preferential to the alternate structure **1b**.

Previously it was ascertained that protonation of **1** occurred principally at N-3″, although minor contributions from other prototropic tautomers could not be discounted (see Scheme 3). As a consequence of protonation at N-3″, the intramolecular hydrogen bonding is no longer in effect and the rotation is essentially uninhibited, comparatively. For the calculations, computations on three species were performed, protonation on N-3″ (**1He**), protonation on N-6 (**1Hg**) and diprotonation on both N-3″ and N-3 (**1H$_2$i**). The calculated energies indicated **1Hg** to be 36 kJ mol^{-1} less stable than **1He** and therefore negligible in concentration. As expected, the torsion angle between the imidazole planes in **1Hg** was quite low, and for both **1H$_2$i** and **1He**, conformers were calculated where the torsion angle remained low.

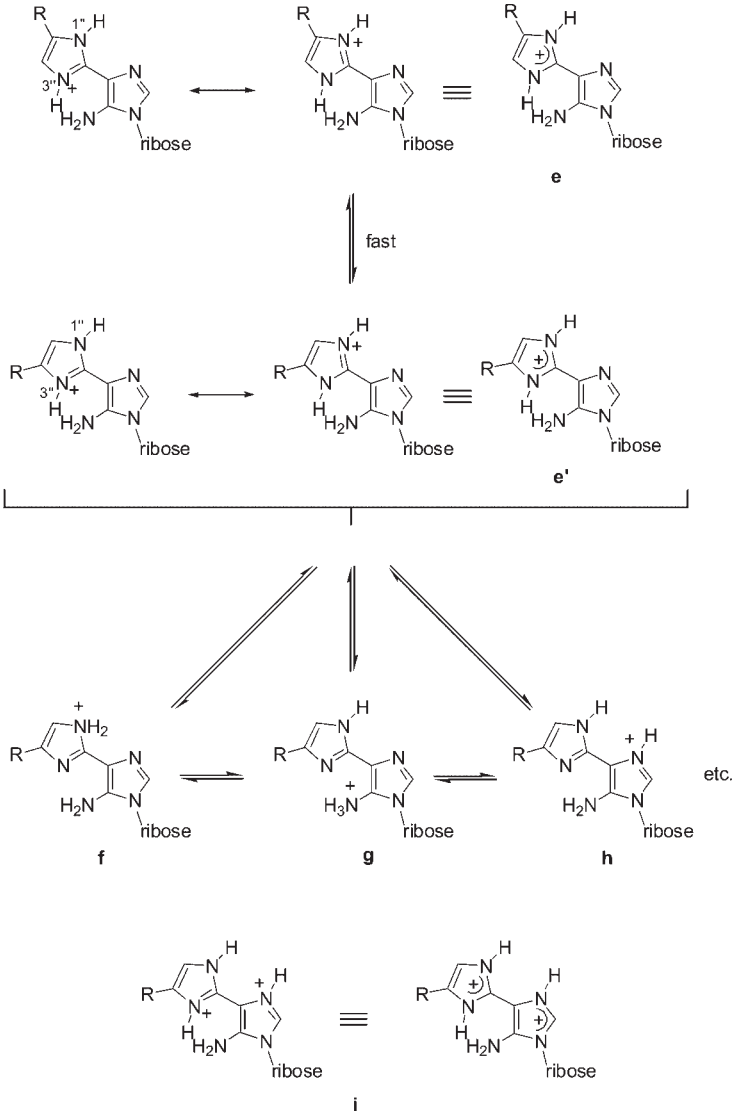

Scheme 3. The various contributing resonance forms of the primary monoprotonated species (**1He**–**3He** and **5He**) and other contributing minor tautomeric forms (**f**–**h**) to the dynamic equilibrium together with the diprotonated species (**i**) observed for the hydroxymethyl (**3H$_2$i**) and oxalo (**4H$_2$i**) substituted derivatives. Rotation about the C_4——$C_{2''}$ bond is essentially unrestricted and preferred roto-tautomers are not inferred for structures incorporating protonation on N-3″ (structures **e**, **i**, etc.)

5-Amino-4-[4″-methylimidazol-2″-yl]-1-(β-D-ribofuranosyl)-1*H*-imidazole (2)

Substitution of the outer imidazole ring changes the dynamics with respect to the restricted rotation and the two roto-tautomers **a** and **d** are no longer equivalent and the exchange process thus amounts to an intramolecular dynamic process consisting of asymmetrical two-site exchange. Compound **2** was found to be particularly well suited and amenable to analysis as the rate of interconversion of the roto-tautomers was slow and both roto-tautomers, **2a** and **2d**, were present in appreciable concentrations. For almost all of the signals of the bi-imidazole moiety of **2**, distinct signals were observed for each of the two roto-tautomers including H-2 and dynamic broadening was even evident on occasion for H-1′ (*vide infra*). The relatively sharp signals observed for the H-4″/H-5″ signals readily facilitated their identification and, although the situation was complicated by spin exchange, NOE enhancements inferred that the NH signal at δ 11.560 (the major roto-tautomer) was adjacent to a methine proton (no NOE was observed from the NH protons to the methyls) and that neither the δ 11.560 nor the δ 11.680 signal was adjacent to NH_2, thereby ruling out structures **2b** and **2c** and providing structure **2a** for the major roto-tautomer and structure **2d** for the minor roto-tautomer by default. The calculated chemical shifts for structures **2a** and **2d** were also a better match for the experimental values in comparison to structures **2b** and **2c**, in particular the C-4″ and C-5″ signals readily provided distinction between **2a** and **2d** thus confirming the structural assignments. Roto-tautomer **2a** was calculated to be $-0.51\,\mathrm{kJ\,mol^{-1}}$ more stable (ΔE) than roto-tautomer **2d**, which is in excellent agreement with

experimental observations (predicted ratio, 55.0 : 45.0; found, 53.5 : 46.5). Similarly, the roto-tautomers **2b** and **2c** were also calculated to be too high in energy to be observable, with similar results being obtained for the pairs of conformers **2b′** and **2b″** and **2c′** and **2c″** with respect to energies, torsion angles, and chemical shifts as was found for the **1b′** and **1b″** conformers.

For **2H**, only one roto-tautomer, **2He**, with a torsion angle of 3.71° was calculated {the differences between the two roto-tautomers is expected to be negligible, as confirmed by the calculation of both the **3He** and **3He′** roto-tautomers (*vide infra*)} and although the agreement between the experimental and calculated chemical shifts was only moderate, it was nonetheless clear that protonation had occurred only at N-3″.

5-Amino-4-[4″-(hydroxymethyl)imidazol-2″-yl]-1-(β-D-ribofuranosyl)-1*H*-imidazole (3)

In the ^{13}C spectra of **3**, only one set of signals was present but a fast exchange process was clearly in evidence as the signals for both C-4″ and C-5″ were severely broadened (and to a lesser extent the CH_2OH carbon), even at 120 °C. In the ^{15}N spectra, neither N-1″ nor N-3″ were observable. To assess whether one of the two likely, intramolecularly hydrogen-bonded forms **3a** and **3d** represents a predominant species for the time-averaged spectra in the absence of both the N-1″ and N-3″ resonances, reliance was placed on the ^{13}C chemical shifts calculated for both **3a** and **3d**. The high-field signal for C-5″ (δ 111.6) implies a proximal disposition to a pyrrole-type nitrogen (N-1″) whilst the low-field signal for C-4″ (δ 139.0) implies that it is adjacent to a pyridine-type nitrogen (N-3″) and based on this the conclusion is drawn that **3a** represents the predominant species in a biased equilibrium. It is not apparent why **3a** is the preferred roto-tautomer in comparison with the methyl derivative **2** where an electron-donating group appears to render little preference for either roto-tautomer. Nothing, though, can be inferred regarding the relative exchange rates as population differences as well as the rate per se affect the appearance of the spectra. The calculations were in full accord with the experimental observations though, as **3a** was predicted to be more stable than **3d** by ca 5.6 kJ mol^{-1} which equates to a predominance of ca 90% at 303 K.

Compound **3H** was isolated from acidic aqueous media (pH 3) and protonation of the pyridine-type nitrogen (N-3″) in the outer imidazole ring was clearly indicated by the chemical shifts of both N-1″ (δ − 219.78) and N-3″ (δ − 218.62). In the ^{13}C spectra, very slight line broadening provided evidence of dynamic effects. Compared with the values for **3a**, the downfield shifts of H-5″ (+0.5 ppm) and C-5″ (+3.4 ppm) and the upfield shifts of, C-2″ (−5.6 ppm) and C-4″ (−6 ppm) all indicated protonation of the outer imidazole ring. In **1H**, both N-1 and N-3 were excluded as the sites of protonation based on the constancy of their chemical shifts in both the unprotonated (**1a**) and protonated (**1H**) forms. For the sample of **3H**, the chemical shift for N-3 (δ − 149.53) is notably upfield by 16.2 ppm in comparison to the value for the unprotonated form **3a** (δ − 133.33). This upfield shift is a clear indication of a degree of protonation at N-3, but for the complete protonation of N-3 the chemical shift would be expected to be at much higher field. Therefore, N-3 is only partially protonated (50% maximum, estimated on the chemical shift of N-3) and the sample thus consists of a mixture of monoprotonated (dominated by **3He**) and diprotonated forms (dominated by $\mathbf{3H_2i}$). As was postulated for **1**,[14] the protonation of the outer imidazole ring also perturbs the chemical shifts of the inner ring atoms by effecting a flow of electrons from the inner ring towards the outer ring. Interestingly, the partial protonation of N-3 in $\mathbf{3H_2}$ resulted in more pronounced effects only in the chemical shifts of C-4 and C-2″, shown by the upfield shifts of −9.4 and −5.6 ppm, in comparison with −7.2 and −4.1 for **1**, respectively.

Previously,[9] no experimental distinction was made between **3** and **3H** and the ^{1}H and ^{13}C chemical shifts for **3** reported in that study are similar to those for **3H** reported here, except for C-4 and C-2″ due to diprotonation. Given the similar manner in which the samples were produced, and since no dynamic exchange broadening was observed, the values obtained in the previous study most likely represent only the mono-protonated species **3H**.

Both **3He** and its rotamer **3He′** were calculated and essentially little difference was found in the chemical shifts for all nuclei and their relative energies. Thus, restricted rotation would not be so easily discernable even if the improbable scenario of a high barrier to rotation was in effect. Thus, the decision to calculate only one structure in the other compounds is justified and the results support the notion of unrestricted, free rotation in the N-3″ protonated species which is adequately represented by **e** alone.

5-Amino-4-[4″-oxaloimidazol-2″-yl]-1-(β-D-ribofuranosyl)-1*H*-imidazole (4)

Given the method of synthesis, it is the sodium salt of the oxalo acid which is the species present in solution and this, of course, has a determinate effect on the exchange rate. For **4**, dynamic exchange effects were also apparent by the line broadening evident for the outer ring carbon signals (C-2″, C-4″ and C-5″) whilst the inner ring nuclei provided sharp signals at their expected chemical shifts (the chemical shifts of the inner ring nuclei are all very similar for **1**–**5**). Due to the dynamic exchange line broadening, only one nitrogen atom in the outer ring was observed, with its chemical shift (δ − 134) indicating it to be a pyridine-type nitrogen and hence it was

assigned as N-3″. This nitrogen also showed a correlation to the proton resonating at δ 7.679, which was thus assigned H-4″. The chemical shift for the methine carbon C-4″ (δ 140.3) also points to it being adjacent to a pyridine-type nitrogen rather than to a pyrrole-type nitrogen. Thus, the restricted rotation about the C_4—$C_{2''}$ bond favors the predominant species **4d**. The observed chemical shifts matched fairly well with the calculated values for species $\mathbf{4d}^-$ although some major deviations were also noted. Also in agreement with the observations, the calculated energies indicated a high preference for $\mathbf{4d}^-$ over $\mathbf{4a}^-$.

Although it appears that the parent compound **1** and the hydroxymethyl derivative **3** are more basic in nature than **4** (and **5**, *vide infra*), isolation of **4H** from an aqueous solution of pH 2 actually resulted in a diprotonated species, $\mathbf{4H_2i}$, with the sites of protonation clearly indicated by the chemical shifts of the nitrogens now bearing the protons. For the diprotonated form of **4H** ($\mathbf{4H_2i}$), N-3 was assigned as one of the sites of protonation as it resonated 55 ppm upfield, in comparison with the unprotonated form **4d**, at $\delta - 188.28$. The chemical shift difference between N-1 and N-3 is therefore reduced markedly to 18 ppm in comparison with 78 ppm for **4d** and indicates a high, if not complete, degree of protonation of N-3. Similarly, the upfield shift for C-4 (−8.9 ppm) and, in particular, the downfield shifts of H-2 by ca 1.2 ppm and H-5″ by ca 0.2 ppm are now of note. It was possible to detect only one ^{15}N NMR signal originating from the outer imidazole ring and this nitrogen, resonating at $\delta - 180.9$, is shifted upfield by −46.7 ppm in comparison with the nitrogen observed for **4d**. From the spectra it is also apparent that rotation about the C_4—$C_{2''}$ bond is almost free although some dynamic process is still in effect. Although the system lies below the coalescence point, the minor species was not detected. Thus whilst protonation clearly occurs at N-3, despite the restricted rotation still in evidence which is complicated by prototropic tautomerism, the chemical shift changes nonetheless imply that protonation has also occurred at N-3″. Initial protonation at N-3 may in fact be preferred due to the electron-withdrawing capability of the oxalyl group by mesomeric effects reducing the basicity of both N-1″ and N-3″. For the most part, the observed chemical shifts fall in between the calculated chemical shifts for the two discrete species **4He** and $\mathbf{4H_2i}$. Furthermore, in comparison to **4H** reported earlier,[9] diprotonation is also indicated by the chemical shift of C-4.

5-Amino-4-[4″-formylimidazol-2″-yl]-1-(β-D-ribofuranosyl)-1*H*-imidazole (5)

For **5**, the predominant species was identified as **5d**, i.e. the same roto-tautomer as observed for **4**, and this can be attributed to the electron-withdrawing capability of the formyl group reducing the basicity of N-3″ in structure **5a** and thereby destabilizing this roto-tautomer relative to structure **5d**. Only the methine carbon in the outer ring (C-4″) shows extreme broadening at room temperature indicating a large chemical shift difference between the two carbons of the different roto-tautomers in comparison with the quaternary carbon C-5″. The reason why this chemical shift difference should be large, or conversely why the chemical shift difference of the quaternary carbon should be small, is not clear. Upon raising the temperature (to 60, 90 °C), the methine carbon clearly sharpens, but other resonances also show distinct sharpening, e.g. the carbon signal of the formyl substituent, C-2″, and to a lesser extent, C-5″ and even C-2 (!). Only one roto-tautomer was actually observed, but these dynamic-exchange broadening effects clearly implicate the presence of a minor roto-tautomer. The structure of the major roto-tautomer was based on the magnitude of the expected $^2J_{H,N}$ and $^3J_{H,N}$ couplings in the outer ring. ^2J between the methine proton and a pyridine-type nitrogen is expected to be large (more than several Hz), whilst the rest should be small, notably ^3J between the methine proton and a pyridine-type nitrogen. Thus with only one correlation present in the HMBC spectrum (based on 8 Hz) between the methine proton and a pyridine-type nitrogen (at $\delta - 129.17$), this places the proton geminal to the pyridine-type nitrogen which is expected to be located near the amine group for the formation of a hydrogen bond resulting in the predominant species **5d**.

Unfortunately, the attempted isolation of **5H** under acidic conditions resulted in problems being encountered with compound solubility and/or stability on all occasions. Inexplicably, the product obtained was sometimes completely insoluble in DMSO and attempts to generate **5H** or $\mathbf{5H_2}$ by the addition of trifluoroacetic acid were also unsuccessful as the compound was readily oxidized or was hydrolysed to the free base and sugar. It was just not a matter of titrating the basic sample and observing spectral simplification as diprotonation also readily occurred in addition to the decomposition and it was simply not possible to obtain spectra for the monoprotonated species only. Thus, experimental evidence cannot be provided for this particular case despite the apparent previous success.[9] However, based on the observations made for **4** and its protonated form it seems feasible that protonation of N-3″ should be accompanied by a high degree or complete protonation of N-3. This seems to be the case for **5H** in the previous study[9] where it was the diprotonated species $\mathbf{5H_2}$ which had in fact been obtained based on the reported ^{13}C chemical shifts, e.g. the upfield shift of C-4.

Final comments and observations

Given that the rate of interconversion between the roto-tautomers is clearly pH dependent, and furthermore, it

was found to also be concentration dependent, it was outside the scope of this study to measure the interconversion rates for samples which displayed rates in the slow-exchange region. Curiously, the interconversion rates were also observed to be time dependent. This phenomenon was previously overlooked due to the manner in which the samples were examined (the NMR samples were normally prepared well in advance of observation) and a freshly made-up sample could display an interconversion rate which increased upon standing up to a final, terminal value. Moreover, it was demonstrated that Na^+ ions could also influence the observed interconversion rate (and the presence of Na^+ ions in both the unprotonated and protonated samples of **2** was readily validated by ^{23}Na NMR), but the exact nature of this interaction and whether Na^+ ion adducts were being formed, was not elucidated. Additional comments and observations on this interesting phenomenon and speculation on the role of Na^+ ions are presented as supplementary material available in EPOC.

The possibility of Na^+ ion adducts being present in solution, however, did not prompt a search by MS as Na^+ ion adducts are often observed under certain MS conditions (e.g. FAB^+, ESI^+, $APCI^+$) as artifacts without pertaining to species actually present in solution. It should be noted though, that solution-state Na^+ adduct species pertaining to real species have been analysed[21] successfully using cold-spray ionization[22] (CSI) and this represents an avenue for further investigation. Attempts were, however, made to obtain additional evidence for the diprotonated species (e.g. $\mathbf{2H_2}$, $\mathbf{3H_2}$) by MS using solutions of the prepared NMR samples as well as solutions of lower pH and by utilizing a variety of sample introduction techniques ($APCI^+$, ESI^+ and FAB^+) in combination with a variety of ion separation systems (sector magnets, ion traps and quadrupoles). The results proved fruitless as none of the conditions provided an identifiable doubly-charged ion, even when conducting fragmentation searches (precursor 'parent' and product 'daughter' ions). But as has been amply demonstrated,[23] gas-phase ions can not only be of opposite charge to the solution-state analytes, but multiply-charged ions can readily be produced from singly-charged species and *vice versa* and the results obtained are heavily dependent on the particular conditions of the analysis.[23]

CONCLUSIONS

Whilst it is not always clear why one roto-tautomer may be preferred over the other, e.g. for **3** roto-tautomer **a** dominates whilst for **2**, the **a** and **d** roto-tautomers are very close in energy, nonetheless excellent agreement between experiment and theory has been obtained. The factors that determine the bias of the equilibrium are the relative electron-withdrawing or -donating capabilities of the R substituent for the imidazole ring in the various roto-tautomers, either by mesomeric or direct inductive effects, and also specifically the electronic influence on N-3″ as this affects the strength of the hydrogen bond and can thus have a marked influence on the overall energy of the structure. The same reasoning as used earlier[14] to identify the roto-tautomers in each case was applied here, no contraindications were found and the same conclusions are drawn but are now supported by theoretical calculations. Thus it has been successfully demonstrated that using GIAO-DFT methodology it is possible to not only determine the site in monoprotonation cases, but also the extent of multiprotonation using ^{15}N NMR spectroscopy and despite the practical shortcomings of ^{15}N NMR, it nevertheless represents an overall advantage, particularly when supported by GIAO-DFT calculations. The same can also be stated with regards to ^{13}C NMR too, particularly when supplemented by calculations. Although the gas phase calculations are good for ^{13}C and ^{15}N whilst only poor for ^{1}H, this is not unexpected given the concentration-dependent behaviour of the ^{1}H chemical shifts and their susceptibility to general environmental influences.

EXPERIMENTAL

NMR spectra were acquired at 30 °C or, where indicated, at elevated temperatures in d_6-DMSO {sample concentrations ca 2, 10, or 100 mg 0.5 ml^{-1} for ^{1}H and 100 mg 0.5 ml^{-1} for ^{13}C, ^{23}Na, and ^{15}N (at natural abundance)} at 11.75 T equipped with either a 5 mm normal configuration tunable probe or a 5 mm inverse *z*-axis field-gradient probe operating at 500.16 MHz for ^{1}H, 125.78 MHz for ^{13}C, 50.69 MHz for ^{15}N, and 132.30 MHz for ^{23}Na. ^{1}H and ^{13}C spectra were referenced internally to the solvent, 2.49 ppm for ^{1}H (to d_5-DMSO) and 39.50 ppm for ^{13}C (to d_6-DMSO); ^{15}N spectra were referenced externally to 90% nitromethane in CD_3NO_2 (0 ppm); ^{23}Na spectra were referenced externally to a saturated solution of NaBr in D_2O (0 ppm). For ^{13}C and ^{15}N, the chemical shifts are reported to two decimal places when taken from 1-D spectra and to one decimal place when they are extracted from the f1 dimension of 2-D spectra or are of very broad resonances in the 1-D spectra. Further general experimental details (NMR and MS), the synthetic methodology[9] (slightly modified) used to obtain compounds **3**–**5** in both their neutral and protonated forms, and the ^{1}H and ^{13}C NMR data for the ribose units of compounds **1** and **3**–**5** are available as supplementary material in EPOC.

Computational methods

Freehand structures were pre-optimized using a molecular mechanics MM^+ method available within the HyperChem program package.[24] Geometry optimizations

were performed using a DFT[18] method contained within the Gaussian 98 program;[25] a B3LYP functional[26] and a 6–31G(d,p) basis set[27] with a tight SCF convergence criterion was used in order to define the structures at a sufficiently high level of theory appropriate[20] for the calculation of reliable NMR shielding constants. The energies of the structures were calculated at the same level of theory. For calculation of the chemical shifts ($\delta = \sigma_{ref.} - \sigma_n$), nuclear shieldings were calculated using the Gaussian 98 program[25] implementation of the GIAO method[17] at the B3LYP/cc-pVTZ level[28] of theory. For calibration of the chemical shifts (^{15}N, ^{13}C and ^{1}H), a range of different compounds (ca 25 in total) were selected encompassing various structural entities and included several substituted pyridines and pyrimidines, several substituted benzenes, naphthalene and other condensed systems, furan, *N*,*N*-dimethyl formamide, nitromethane, TMS, and the aliphatic heterobicyclic systems of refs 29 and 30 amongst others. The geometries of the selected calibration compounds were optimized and their chemical shifts calculated using the same methodology as for the compounds under study; their experimental chemical shifts were either measured or taken from refs 20, 29, or 30 and plotted *vs* the calculated shifts (see Figs 1–3). The resulting sum of the least squares method fitted linear equations were then used to calibrate the calculated chemical shifts of the studied compounds for comparison with the experimental values.

Syntheses

The preparation of the starting ethenoadenosines and the structural characterization of the bi-imidazole nucleosides **1** and **3–5** resulting from ring-opening have been described in detail previously[9] but the methodology to obtain the substituted bi-imidazoles **3–5** in both their neutral and protonated forms has been slightly modified and is described in the supplementary material available in EPOC together with the ^{1}H and ^{13}C NMR data for the ribose units of compounds **1** and **3–5**.

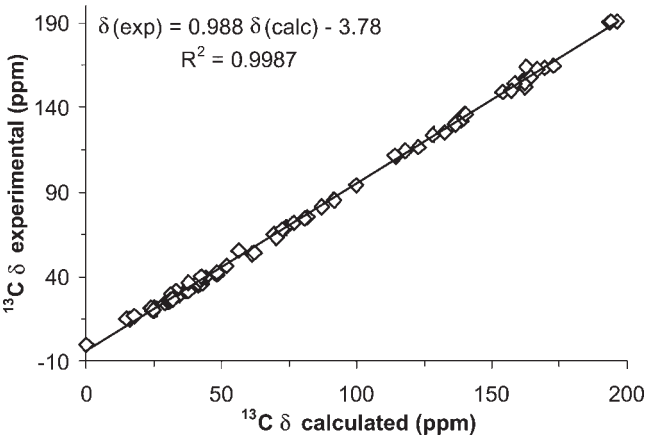

Figure 2. Plot of GIAO-DFT {B3LYP/cc-pVTZ}-calculated vs experimentally observed ^{13}C NMR chemical shifts for a range of compounds and nuclear environments

5-Amino-4-[4″-methylimidazol-2″-yl]-1-(β-D-ribofuranosyl)-1*H*-imidazole (2) and its protonated form (2H)

7-Methylethenoadenosine, prepared according to the method of Virta *et al.*,[31] (0.85 g, 2.78 mmol) was heated for 15 h at 80 °C in 100 ml of 0.1 M NaOH. After cooling to room temperature, the mixture was divided into two equal portions. One half of the mixture was concentrated to a volume of ca 20 ml by rotary evaporation and stored in a refrigerator for overnight. The crystalline material was filtered off, redissolved in 10 ml of 0.05 M NaOH and again stored overnight in a refrigerator to yield a crystalline product. The product was collected by filtration and dried in a vacuum desiccator over diphosphorus pentoxide to afford the neutral form of **2** (0.15 g, 37%) as a white powder. UV: $\lambda_{max}(H_2O)$/nm

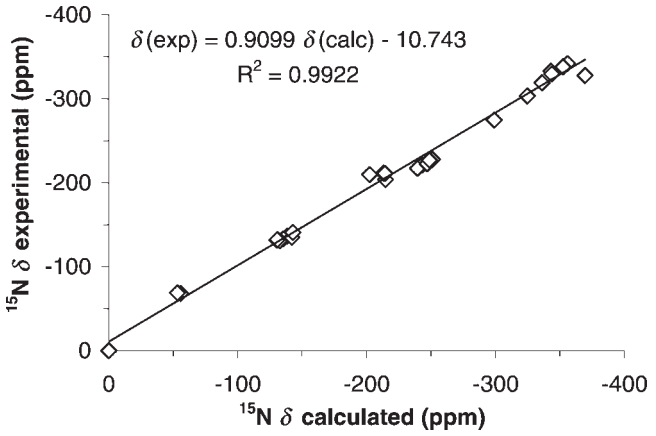

Figure 1. Plot of GIAO-DFT {B3LYP/cc-pVTZ}-calculated vs experimentally observed ^{15}N NMR chemical shifts for a range of compounds and nuclear environments

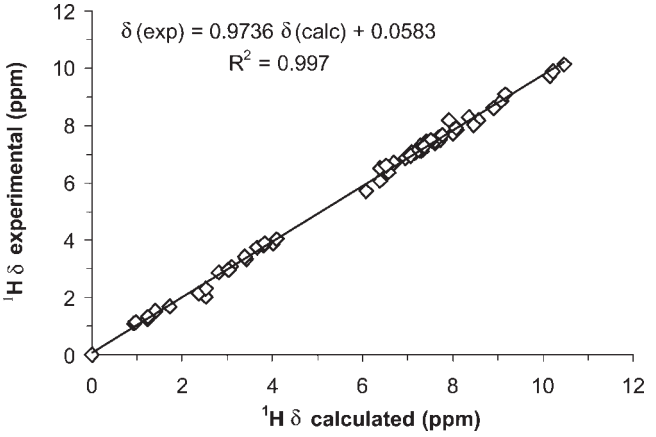

Figure 3. Plot of GIAO-DFT {B3LYP/cc-pVTZ}-calculated vs experimentally observed ^{1}H NMR chemical shifts for a range of compounds and nuclear environments

216, 280; $\lambda_{min}(H_2O)$/nm 234. *m/z* (FAB^+) 296 (MH^+, 100%), 164 (MH^+ − ribosyl + H, 100%). HRMS (FAB^+) (MH^+) 296.1331 (calcd. for $C_{12}H_{18}N_5O_4$: 296.1359). For the ^1H, ^{13}C and ^{15}N NMR of the imidazole rings, see Tables S1 and S2. For the ribose unit of **2**, the spectra of both roto-tautomers were isochronous and only one set of signals was observed. ^1H NMR (conc soln) δ ppm: 5.520 (d, $J_{H\text{-}2'} = 6.2$, H-1′), 4.357 (t, $J_{H\text{-}1'} = J_{H\text{-}3'} = 5.8$, H-2′), 4.106 (dd, $J_{H\text{-}2'} = 5.1$, $J_{H\text{-}4'} = 3.4$, H-3′), 3.923 (∼qt, $J_{H\text{-}3'} = J_{H\text{-}5a'} = J_{H\text{-}5b'} = 3.3$, H-4′), 3.638 (d(AB)d, $J_{H\text{-}5b'} = -11.9$, $J_{H\text{-}4'} = 3.3$, H-5a′), 3.605 (d(AB)d, $J_{H\text{-}5a'} = -11.9$, $J_{H\text{-}4'} = 3.2$, H-5b′), 5.401 and 5.260 (br s, HO-2′, HO-3′, HO-5′), (10 mg 0.5 ml^{-1} soln) 5.486 (d, $J_{H\text{-}2'} = 6.2$, H-1′), 4.323 (t, $J_{H\text{-}1'} = J_{H\text{-}3'} = 5.8$, H-2′), 4.069 (m, H-3′), 3.886 (∼qt, $J_{H\text{-}3'} = J_{H\text{-}5a'} = J_{H\text{-}5b'} = 3.2$, H-4′), 3.615 (d(AB)d,$J_{H\text{-}5b'} = -12.2$, $J_{H\text{-}4'} = 3.0$, H-5a′), 3.574 (d(AB)d, $J_{H\text{-}5a'} = -12.1$, $J_{H\text{-}4'} = 3.0$, H-5b′), 5.358 and 5.189 (br s, HO-2′, HO-3′, HO-5′), and (dilute soln) 5.475 (d, $J_{H\text{-}2'} = 6.2$, H-1′), 4.311 (∼qt, $J_{H\text{-}1'} = 6.2$, $J_{H\text{-}3'} = 4.7$, $J_{HO\text{-}2'} = 6.2$, H-2′), 4.062 (∼qt, $J_{H\text{-}2'} = 4.7$, $J_{H\text{-}4'} = 3.3$, $J_{HO\text{-}3'} = 4.3$, H-3′), 3.878 (∼qt, $J_{H\text{-}3'} = 3.3$, $J_{H\text{-}5a'} = 3.3$, $J_{H\text{-}5b'} = 3.3$, H-4′), 3.603 (m, $J_{H\text{-}5b'} = -12.0$, $J_{H\text{-}4'} = 3.3$, $J_{HO\text{-}5'} = 4.9$, H-5a′), 3.569 (m, $J_{H\text{-}5a'} = -12.0$, $J_{H\text{-}4'} = 3.3$, $J_{HO\text{-}5'} = 4.6$, H-5b′), 5.317 (d, $J_{H\text{-}2'} = 6.2$, HO-2′), 5.153 (t, $J_{H\text{-}5a'} = 4.9$, $J_{H\text{-}5b'} = 4.6$, HO-5′), 5.116 (d, $J_{H\text{-}3'} = 4.3$, HO-3′). ^{13}C NMR (conc soln) δ ppm: 87.91 (sl br, C-1′), 85.22 (C-4′), 73.11 (sl br, C-2′), 70.23 (C-3′), 61.22 (C-5′).

The other half of the reaction mixture from above was acidified to pH 4 by the addition of dilute HCl. The mixture was concentrated to a volume of ca 10 ml and acetone–diethyl ether (1 : 2 v/v) added until the mixture became cloudy. Storage of the mixture in a refrigerator overnight afforded a crystalline product which was filtered off, redissolved in 5 ml of water and the pH of the resulting solution again adjusted to pH 4 by the addition of dilute HCl. The product was precipitated under cold conditions by the addition of acetone–Et_2O (1 : 2 v/v), collected by filtration, and dried in a vacuum desiccator over diphosphorus pentoxide to afford the protonated form of **2** (0.19 g, 47%) as a white powder. For the ^1H, ^{13}C and ^{15}N NMR of the imidazole rings, see Tables S1 and S2. For the ribose unit of **2H**, ^1H NMR (conc soln) δ ppm: 5.576 (d, $J_{H\text{-}2'} = 6.3$, H-1′), 4.291 (t, $J_{H\text{-}1'} = J_{H\text{-}3'} = 5.7$, H-2′), 4.090 (dd, $J_{H\text{-}2'} = 5.1$, $J_{H\text{-}4'} = 3.2$, H-3′), 3.941 (∼qt, $J_{H\text{-}3'} = J_{H\text{-}5a'} = J_{H\text{-}5b'} = 3.0$, H-4′), 3.605 (d(AB)d, $J_{H\text{-}5b'} = -12.5$, $J_{H\text{-}4'} = 3.0$, H-5a′), 3.590 (d(AB)d, $J_{H\text{-}5a'} = -12.7$, $J_{H\text{-}4'} = 3.0$, H-5b′), (the signals of the HO-2′, HO-3′ and HO-5′ protons were not observed), (10 mg 0.5 ml^{-1} soln) 5.556 (d, $J_{H\text{-}2'} = 6.5$, H-1′), 4.298 (t, $J_{H\text{-}1'} = J_{H\text{-}3'} = 5.3$, H-2′), 4.065 (dd, $J_{H\text{-}2'} = 5.0$, $J_{H\text{-}4'} = 3.1$, H-3′), 3.933 (∼qt, $J_{H\text{-}3'} = J_{H\text{-}5a'} = J_{H\text{-}5b'} = 3.0$, H-4′), ∼3.60 (d(AB)d, $J_{H\text{-}5b'} = -11.7$, $J_{H\text{-}4'} = 2.8$, H-5a′), ∼3.58 (d(AB)d, $J_{H\text{-}5a'} = -11.5$, $J_{H\text{-}4'} = 2.7$, H-5b′), 5.476, 5.363, 5.219 (br s, HO-2′, HO-3′ and HO-5′), and (dilute soln) 5.560 (d, $J_{H\text{-}2'} = 6.4$, H-1′), 4.294 (t, $J_{H\text{-}1'} = 6.4$, $J_{H\text{-}3'} = 5.2$, H-2′), 4.071 (dd, $J_{H\text{-}2'} = 5.2$, $J_{H\text{-}4'} = 3.1$, H-3′), 3.936 (∼qt, $J_{H\text{-}3'} = 3.1$, $J_{H\text{-}5a'} = 3.1$, $J_{H\text{-}5b'} = 3.0$, H-4′), 3.606 (d(AB)d, $J_{H\text{-}5b'} = -12.0$, $J_{H\text{-}4'} = 3.1$, H-5a′), 3.589 (d(AB)d, $J_{H\text{-}5a'} = -12.0$, $J_{H\text{-}4'} = 3.0$, H-5b′), 5.468, 5.342, 5.192 (br s, HO-2′, HO-3′, HO-5′). ^{13}C NMR (conc soln) δ ppm: 88.01 (C-1′), 85.62 (C-4′), 73.12 (C-2′), 70.13 (C-3′), 60.96 (C-5′).

Acknowledgements

The assistance of Mr Markku Reunanen (Åbo Akademi University) with the FAB MS analyses is gratefully acknowledged. The authors also thank the Center for Scientific Computing (CSC, Finland) for a generous allocation of computational time.

REFERENCES

1. (a) Cadet J, Bourdat A-G, D'Ham C, Duarte V, Gasparutto D, Romieu A, Ravanat J-L. *Mutat. Res.* 2000; **462**: 121–128; (b) Speina E, Cieśla JM, Wójcik J, Bajek M, Kuśmierek JT, Tudek B. *J. Biol. Chem.* 2001; **276**: 21821–21827; (c) Burgdorf LT, Carell T. *Chem. Eur. J.* 2002; **8**: 293–301; (d) Haraguchi K, Delaney MO, Wiederholt CJ, Sambandam A, Hantosi Zs, Greenberg MM. *J. Am. Chem. Soc.* 2002; **124**: 3263–3269; (e) Delaney MO, Wiederholt CJ, Greenberg MM. *Angew. Chem. Int. Ed.* 2002; **41**: 771–773; (f) Saparbaev M, Langouët S, Privezentzev CV, Guengerich FP, Cai H, Elder RH, Laval J. *J. Biol. Chem.* 2002; **277**: 26987–26993.
2. (a) Harris CC. *Cancer Res.* 1991; **51**: 5023s–5044s; (b) Ames BN, Shigenaga MK, Hagen TM. *Proc. Natl. Acad. Sci. USA* 1993; **90**: 7915–7922; (c) Dipple A. *Carcinogenesis* 1995; **16**: 437–441; (d) Gupta RC, Lutz WK. *Mutat. Res.* 1999; **424**: 1–8; (e) Marnett LJ, Plastaras JP. *Trends Genet.* 2001; **17**; 214–221.
3. (a) Leonard NJ. *CRC Crit. Rev. Biochem.* 1984; **15**: 125–199; (b) Nair J, Barbin A, Velic I, Bartsch H. *Mutat. Res.* 1999; **424**: 59–69; (c) Barbin A. *Mutat. Res.* 2000; **462**: 55–69.
4. (a) Bartsch H, Barbin A, Marion M-J, Nair J, Guichard Y. *Drug Metab. Rev.* 1994; **26**: 349–371; (b) Burcham PC. *Mutagenesis* 1998; **13**: 287–305.
5. (a) Barbin A, Bartsch H, Leconte P, Radman M. *Nucleic Acids Res.* 1981; **9**: 375–387; (b) Spengler S, Singer B. *Nucleic Acids Res.* 1981; **9**: 365–373.
6. Swenberg JA, Fedtke N, Ciroussel F, Barbin A, Bartsch H. *Carcinogenesis* 1992; **13**: 727–729.
7. (a) Nair V, Offerman RJ, Turner GA. *J. Org. Chem.* 1984; **49**: 4021–4025; (b) Golding BT, Slaich PK, Watson WP. *J. Chem. Soc. Chem. Comm.* 1986; 515–517; (c) Kronberg L, Sjöholm R, Karlsson S. *Chem. Res. Toxicol.* 1992; **5**: 852–855; (d) Kronberg L, Karlsson S, Sjöholm R. *Chem. Res. Toxicol.* 1993; **6**: 495–499; (e) Mäki J, Sjöholm R, Kronberg L. *J. Chem. Soc. Perkin Trans. 1* 1999; 2923–2928.
8. (a) Yip KF, Tsou KC. *Tetrahedron Lett.* 1973; 3087–3090; (b) Tsou KC, Yip KF, Miller EE, Lo KW. *Nucleic Acids Res.* 1974; **1**: 531–547.
9. Mäki J, Sjöholm R, Kronberg L. *J. Chem. Soc. Perkin Trans. 1* 2000; 4445–4450.
10. Claramunt RM, Santa María MD, Infantes L, Cano FH, Elguero J. *J. Chem. Soc. Perkin Trans. 2* 2002; 564–568.
11. Kalinowski HO, Berger S, Braun S. In *Carbon-13 NMR Spectroscopy.* Wiley: Chichester, 1988.
12. Berger S, Braun S, Kalinowski HO. In *NMR Spectroscopy of the Non-Metallic Elements*. Wiley: Chichester, 1997, English Edition, Ch. 4.
13. Major DT, Laxer A, Fischer B. *J. Org. Chem.* 2002; **67**: 790–802.
14. Mäki J, Klika KD, Sjöholm R, Kronberg L. *J. Chem. Soc. Perkin Trans. 1* 2001; 1216–1219.

15. Cmoch P, Stefaniek L, Melzer E, Baloniak S, Webb GA. *Magn. Reson. Chem.* 1999; **37**: 493–497.
16. Bagno A, Scorrano G. *Acc. Chem. Res.* 2000; **33**: 609–616.
17. Wolinski K, Hinton JF, Pulay P. *J. Am. Chem. Soc.* 1990; **112**: 8251–8260.
18. (a) Hohenberg P, Kohn W. *Phys. Rev. B* 1964; **136**: 864–871; (b) Kohn W, Sham LJ. *Phys. Rev. A* 1965; **140**: 1133–1138; (c) Parr RG, Yang W. In *Density Functional Theory Of Atoms And Molecules*. Oxford Science Publishers: New York, 1989.
19. Arpalahti J, Klika KD. *Eur. J. Inorg. Chem.* 1999; 1199–1201.
20. Bagno A. *Chem. Eur. J.* 2001; **7**: 1652–1661.
21. Sakamoto S, Nakatani K, Saito I, Yamaguchi K. *J. Chem. Soc. Chem. Comm.* 2003; 788–789.
22. Sakamoto S, Fujita M, Kim K, Yamaguchi K. *Tetrahedron* 2000; **56**: 955–964.
23. Iavarone AT, Williams ER. *J. Am. Chem. Soc.* 2003; **125**: 2319–2327 and references cited therein.
24. HyperChem Release 4.5 for Windows, Hypercube Inc., 1995.
25. Frisch MJ, Trucks GW, Schlegel HB, Scuseria GE, Robb MA, Cheeseman JR, Zakrzewski VG, Montgomery JA Jr, Stratmann RE, Burant JC, Dapprich S, Millam JM, Daniels AD, Kudin KN, Strain MC, Farkas O, Tomasi J, Barone V, Cossi M, Cammi R, Mennucci B, Pomelli C, Adamo C, Clifford S, Ochterski J, Petersson GA, Ayala PY, Cui Q, Morokuma K, Malick DK, Rabuck AD, Raghavachari K, Foresman JB, Cioslowski J, Ortiz JV, Stefanov BB, Liu G, Liashenko A, Piskorz P, Komaromi I, Gomperts R, Martin RL, Fox DJ, Keith T, Al-Laham MA, Peng CY, Nanayakkara A, Gonzalez C, Challacombe M, Gill PMW, Johnson BG, Chen W, Wong MW, Andres JL, Head-Gordon M, Replogle ES, Pople JA. *Gaussian 98*, *Revision A.11*. Gaussian: Pittsburgh, PA, 2001.
26. (a) Becke AD. *Phys. Rev. A* 1988; **38**: 3098–3100; (b) Becke AD. *J. Chem. Phys.* 1993; **98**: 5648–5652; (c) Lee C, Yang W, Parr RG. *Phys. Rev. B* 1988; **37**: 785–789; (d) Miehlich B, Savin A, Stoll H, Preuss H. *Chem. Phys. Lett.* 1989; **157**: 200–206.
27. Hehre WJ, Radom L, vR Schleyer P, Pople JA. In *Ab Initio Molecular Orbital Theory*. Wiley: New York, 1986.
28. Kendall RA, Dunning TH Jr, Harrison RJ. *J. Chem. Phys.* 1992; **96**: 6796–6806.
29. Tähtinen P, Sinkkonen J, Klika KD, Nieminen V, Stájer G, Szakonyi Zs, Fülöp F, Pihlaja K. *Chirality* 2002; **14**: 187–198.
30. Tähtinen P, Bagno A, Klika KD, Pihlaja K. *J. Am. Chem. Soc.* 2003; **125**: 4609–4618.
31. Virta P, Holmström T, Munter T, Nyholm T, Kronberg L, Sjöholm R. *Nucleos. Nucleot. Nucl.* 2003; **22**: 85–98.